

In vivo non-thermal irreversible electroporation impact on rat liver galvanic apparent internal resistance

This article has been downloaded from IOPscience. Please scroll down to see the full text article.

2011 Phys. Med. Biol. 56 951

(<http://iopscience.iop.org/0031-9155/56/4/005>)

View [the table of contents for this issue](#), or go to the [journal homepage](#) for more

Download details:

IP Address: 156.18.70.5

The article was downloaded on 10/02/2011 at 17:43

Please note that [terms and conditions apply](#).

***In vivo* non-thermal irreversible electroporation impact on rat liver galvanic apparent internal resistance**

A Golberg^{1,4}, S Laufer^{1,4}, H D Rabinowitch^{2,5} and B Rubinsky³

¹ Center for Bioengineering in the Service of Humanity and Society, School of Computer Science and Engineering, The Hebrew University of Jerusalem, Jerusalem 91904, Israel

² Robert H Smith Faculty of Agriculture, Food and Environment, Robert H Smith Institute of Plant Science and Genetics in Agriculture, Hebrew University of Jerusalem, Rehovot 76 100, Israel

³ Department of Mechanical Engineering, Graduate Program in Biophysics, University of California at Berkeley, Berkeley, CA 84720, USA

E-mail: Rabin@agri.huji.ac.il

Received 1 September 2010

Published 19 January 2011

Online at stacks.iop.org/PMB/56/951

Abstract

Non-thermal irreversible electroporation (NTIRE) is a biophysical phenomenon which involves application of electric field pulses to cells or tissues, causing certain rearrangements in the membrane structure leading to cell death. The treated tissue ac impedance changes induced by electroporation were shown to be the indicators for NTIRE efficiency. In a previous study we characterized *in vitro* tissue galvanic apparent internal resistance (GAIR) changes due to NTIRE. Here we describe an *in vivo* study in which we monitored the GAIR changes of a rat liver treated by NTIRE. Electrical pulses were delivered through the same Zn/Cu electrodes by which GAIR was measured. GAIR was measured before and for 3 h after the treatment at 15 min intervals. The results were compared to the established ac bioimpedance measurement method. A decrease of 33% was measured immediately after the NTIRE treatment and a 40% decrease was measured after 3 h in GAIR values; in the same time 40% and 47% decrease respectively were measured by ac bioimpedance analyses. The temperature increase due to the NTIRE was only 0.5 °C. The results open the way for an inexpensive, self-powered *in vivo* real-time NTIRE effectiveness measurement.

(Some figures in this article are in colour only in the electronic version)

⁴ Authors made equal contribution to the work.

⁵ Author to whom any correspondence should be addressed.

1. Introduction

Certain strong electrical fields cause cell membrane permeabilization due to nano-scale perforations (Rubinsky 2007), commonly named ‘electroporation’ (Rubinsky 2007). Under certain conditions, non-thermal irreversible electroporation (NTIRE) leads to non-thermal cell death (Rubinsky 2010).

For four decades NTIRE has been applied for microbial inactivation mainly by the food industry (Barbosa-Cánovas *et al* 1999, FDA 2000, Lelieveld *et al* 2007), and lately it was proposed for drug disinfection (Golberg *et al* 2009a). Summaries on recent advances are available (Golberg *et al* 2010a, Lelieveld *et al* 2007).

The use of irreversible electroporation in a non-thermal mode for *in vivo* tissue ablation is a new, minimally-invasive molecular-selective surgical technique (Rubinsky 2010), where electrodes in contact with the target tissue deliver electric pulses for NTIRE induction (Edd *et al* 2006, Rubinsky 2007) with the consequent of rupture membranes. Other cell structures remain intact and the neighboring cells are not affected (Edd and Davalos 2007, Rubinsky 2007). Hence, pulses of specific amplitude and frequency generated by the electrodes inserted into the periphery of malignant tissue destroy only the cancerous cells (Rubinsky 2010). The medical success of the treatment depends on complete ablation of the treated tissue, and therefore real-time feedback information is crucial for the clinical application of this minimally invasive technique (Thomson 2010).

Several measuring methods of NTIRE impact have been proposed, including ultrasound, MRI and CT (Guo *et al* 2010, Lee *et al* 2010, 2007). These techniques, however, require state-of-the-art infrastructure and additional sophisticated and expensive equipment. Alternative techniques are based on measuring the tissue’s electrical properties (Cukjati *et al* 2007, Dev *et al* 2003, Glahder *et al* 2005, Ivorra *et al* 2009, Ivorra and Rubinsky 2007). These techniques, however, are costly and require calibration of the relevant measuring devices.

Employing basic galvanic battery principles, we characterized the electricity generation capacity of tissues through electrolysis, and proposed to apply this independent external-power-source system for driving implanted medical devices (Golberg *et al* 2009b, 2010b). *In vitro* research on Zn/Cu electrolysis in various animal organs revealed a basic and tissue-specific measurable property, the galvanic apparent internal resistance (GAIR) (Golberg *et al* 2009b). This property appears to be fundamental and is most likely related to the electrodes’ delineated tissue’s function as a salt bridge. Unlike other tissue electrical traits (Foster and Schwan 1989, Gabriel and Gabriel 1996, Gabriel *et al* 1996, Grimnes and Martinsen 2000) GAIR represents an easy to measure electrical property of the tissue, independent of external power supply. GAIR measurements thus provide insight into the basic mechanisms that control the interactions of electric fields within live tissues.

The potential advantage of GAIR as a self-powered electrochemical diagnostic method for efficient measurement of the NTIRE effects *in vitro* (Golberg *et al* 2009b) encouraged us to measure GAIR values *in vivo*. This work was undertaken to characterize the effect of the NTIRE protocol on GAIR values.

2. Materials and methods

The key objective of this study is to obtain a fundamental understanding of the NTIRE effects on GAIR performance *in vivo*. Additionally, we studied the long-term effects of NTIRE treatment on both GAIR and ac bioimpedance values *in vivo*.

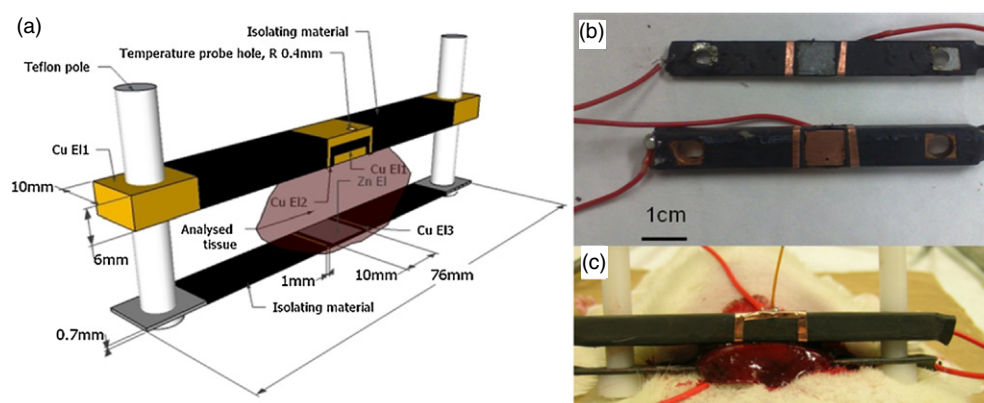


Figure 1. Electroporation and impedance measurement electrode set-up. The exposed liver lobe was placed between the two electrodes (each having 1 cm^2 working area). The distance between the electrodes was determined solely by the thickness of the treated tissue. Two Teflon poles allowed free sliding of the top electrode. (a) Schematic representation of the four electrode set-up (a pair of Cu/Zn plates plus two Cu strips); (b) actual electrode set-up for four-electrode bioimpedance measurement and NTIRE pulse delivery; (c) electrodes positioned on animal's abdomen during the procedure.

2.1. Electrode design

A pair of Zn/Cu electrodes was employed for NTIRE pulse delivery, and for measuring both ac impedance and GAIR (figure 1). The dimensions and weight of the Cu and Zn electrodes were $76 \text{ mm} \times 6 \text{ mm} \times 10 \text{ mm}$ and $76 \text{ mm} \times 0.7 \text{ mm} \times 10 \text{ mm}$, and 36 and 4 g, respectively (CuEI1 and ZnEI, figure 1(a)). For each of the above electrodes, a 1 cm^2 working surface area was exposed. In addition, the four-electrode method was employed for ac impedance measurements (Ivorra *et al* 2009, Ivorra and Rubinsky 2007), using two 1 mm thick Cu electrodes (CuEI2, CuEI3; figure 1(a)) with 0.1 cm^2 working surface attached to the insulation material. Two Teflon poles were tightened to the bottom electrode (ZnEI, figure 1(a)), while the top electrode (CuEI1, figure 1(a)) was free to slide vertically on the poles, driven by its own weight. Hence, the distance between the electrodes was self-adjusted according to the thickness of the treated tissue. The entire set-up was placed on the animal abdomen, thus allowing its movement in tandem with the animal breathing. For temperature measurement a 0.8 mm diameter hole was drilled in the top electrode. (CuEI1).

2.2. Animal procedures

Male Sprague-Dawley rats (340–360 g) (Harlan Laboratories, Jerusalem, Israel) received humane care from a properly trained professional. All procedures complied with the National Institute of Health Guide for the Care and Use of Laboratory Animals, and were approved by the Institutional Animal Care and Use Committee of the Hebrew University. Prior to any intervention, the animal was anesthetized employing intraperitoneal injection of Ketamine (Ketaset[®] 100 mg ml^{-1} , Fort Dodge Animal Health, USA) at 100 mg kg^{-1} , and medetomidin (Domitor 1 mg ml^{-1} OrionPharma, Finland) at 0.8 mg kg^{-1} of rat body weight. Only after full anesthesia was achieved, was the liver exposed by midline incision. One liver lobe was placed between the two Cu/Zn electrodes plates for NTIRE treatment, and GAIR and bioimpedance measurements. At the end of the experiment the animal was sacrificed. Control animals were treated similarly with the exception of the NTIRE treatment.

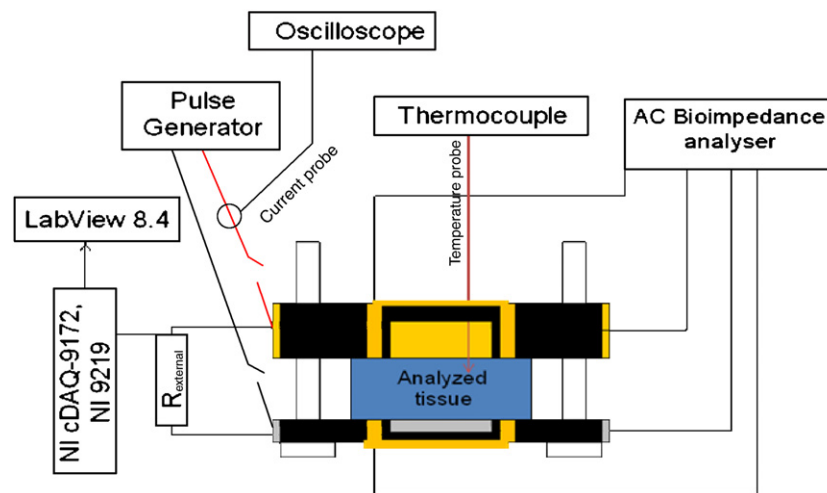


Figure 2. Schematic presentation of the *in vivo* experimental set-up. Including NTIRE treatment, and GAIR ac bioimpedance and temperature measurements.

2.3. Electroporation

For tissue ablation Zn and three Cu electrodes were connected to an electroporator power supply (BTX 830, Harvard Apparatus, Holliston, MA, USA) (figure 2). A single NTIRE treatment consisting of 90 unipolar, rectangular electric $70 \mu\text{s}$ pulses, were delivered at 150 V mm^{-1} electric field, 4 Hz (Rubinsky 2010).

2.4. Galvanic resistance measurement

GAIR was measured immediately before electroporation and every 15 min thereafter, for 3 h, as previously described (Golberg *et al* 2009b). In brief, a galvanic cell was constructed by sandwiching the analyzed tissue between Zn and Cu electrodes (figure 2). The cell was discharged over a series of 3Ω to $100 \text{ k}\Omega$ external resistors (R_{ext}), and the generated voltage was measured by a voltmeter (NI cDAQ-9172, NI 9219 plug, National Instruments Ltd, Austin, TX, USA) connected in parallel to the variable resistors. The operational system was controlled by custom written software (Labview, version 8.4 National Instruments Ltd, Austin, TX, USA). Control animals were treated similarly excluding the NTIRE pulses.

2.5. Bioimpedance

AC bioimpedance was measured using the four-electrode method (Ivorra *et al* 2009, Ivorra and Rubinsky 2007) as follows. The Zn and Cu electrodes were employed for current injection (maximum current $100 \mu\text{A}$), while two, 1 mm thick Cu strips served for voltage measurement (figure 1). In the NTIRE procedure, the two strips also served to guarantee electroporation throughout the tissue's treated volume. The impedance was measured using a 4-wire bioimpedance meter developed by i2m Design SA (Guimerà *et al* 2009). Twenty logarithmically spaced frequencies, ranging between 100 and 1 MHz, were measured immediately before the NTIRE treatment and thereafter at 30 min intervals up to 3 h. Ten consecutive readings were taken at each measuring time.

2.6. Temperature

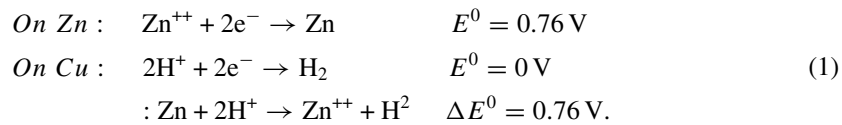
Tissue temperature measurements were taken before, during and after the electroporation procedure using Reflex Signal Conditioner with polyimide covered 0.7 mm probe (Neoptix, Inc., Québec, Canada). The probe was inserted into the tissue 1 mm below the Cu electrode (figures 1 and 2).

2.7. Histology

Treated and control liver lobes were removed from the sacrificed animals and immediately stored in formaldehyde solution. Morphological studies of the treated and control tissues were made following hematoxylin-eosin staining (Patho-Lab Diagnostics Research Unit, Nes Ziona, Israel) of cross sections sampled from the center of the livers' treated regions.

2.8. GAIR values *in vivo*

The GAIR values of exposed liver lobes were systematically calculated from the measured voltage generated as a function of the external resistance values across the electrodes. We have previously shown that the Zn/Cu tissue galvanic cell primary mechanism of voltage production is electrolysis, where the tissue functions as a typical salt bridge between the two electrodes (Golberg *et al* 2009b, 2010b). The structure of such a galvanic cell suggests that oxidation of the Zn electrode occurs while hydrogen is being reduced at the Cu electrode surface area (Vanysek 2007), as depicted in equation (1):



Hence, this organic-cell can be modeled using standard galvanic battery characterization techniques (Kiehne 2003) and consequently generate voltage with an open circuit value of 0.76 V in series with a GAIR of the salt bridge, R_{app} . Employing the previously described methodology (Golberg *et al* 2010b) we examined the relationship between current density and voltages. On circuit closing by an external resistance R_{ext} (figure 1), R_{app} value can be estimated from the measured current— I_d (equation (2)), provided that the galvanic internal (impedance) resistivity (GAIR) is normalized to the cell geometry (Kiehne 2003):

$$\begin{aligned} \frac{1}{I_d} &= \frac{R_{\text{ext}}}{\text{OCV}} + \frac{R_{\text{app}}}{\text{OCV}} \\ \text{GAIR} &= R_{\text{app}} * K_{\text{cell}} (\Omega \text{ cm}). \end{aligned} \quad (2)$$

where i_d (A cm^{-2}) is the calculated current density; R_{ext} (Ω) is the variable external resistance; R_{app} (Ω) is the internal resistance of a galvanic cell; OCV (V) is the open circuit voltage; K_{cell} ($\Omega \text{ cm}$) is the cell constant, which is the quotient between the active electrode surface area and the distance between the electrodes, and GAIR is the apparent internal resistance of the tissue galvanic cell.

2.9. AC bioimpedance analyses

For the parameterization of the frequency-dependent impedance, the Cole dispersion model (Halter *et al* 2008, Kenneth and Robert 1941) was employed (equation (3)):

$$Z(f) = R_{\infty} + \frac{R_0 - R_{\infty}}{1 + \left(\frac{if}{f_c}\right)^{\alpha}}, \quad (3)$$

where $Z(f)$ (Ω) is the complex resistivity at frequency f (Hz). R_∞ is the high frequency resistivity that correlates with the cumulative intracellular and extracellular resistivity. R_0 is the low frequency resistivity that is associated with the extracellular resistivity. f_c is the characteristic frequency related to cell membrane quantity and viability as estimated by the Cole–Cole model (see below) from impedance measurements; α is the fractional power resulting from the depression of the circular arc from the x -axis representing tissue heterogeneity (Halter *et al* 2009).

The four parameters (R_0 , R_∞ , f_c , and α) were estimated with MATLAB's (The MathWorks, Natick, MA, USA) function *fsolve* using the Levenberg–Marquardt method (Marquardt 1963, Moré 1978). The quality of the estimates was evaluated using the goodness criterion (Halter *et al* 2008) given in equation (4):

$$\varepsilon = \frac{1}{N} \sum_{i=1}^N |Z_m(f_i) - Z_e(f_i)|, \quad (4)$$

where $Z_m(f_i)$ and $Z_e(f_i)$ are the measured and estimated impedances at each frequency, respectively, and N is the number of frequencies.

2.10. Statistics

Statistical analyses were performed using the Microsoft Office Excel 2007 external package, and paired one-tailed Student t -tests.

3. Results

IRE was performed on five animals and an additional five animals were used for control.

Temperature measurements showed a 0.5 °C increase of liver temperatures after the NTIRE procedure, while the liver temperature of control animals remained unchanged.

3.1. GAIR measurement

In agreement with our *in vitro* findings with plants (Golberg *et al* 2010b) and animals (Golberg *et al* 2009b), our data show a highly linear relationship between the external resistance R_{ext} and $1/i_d$ (unpublished), thus supporting our hypothesis that living tissue-based galvanic cells function as an ohmic resistance battery over a wide range of external loads, *in vivo*.

Liver lobes vary in dimensions, thus the distance between the Cu and Zn plate electrodes varied from 3.6 to 5.3 mm. Consequently, K_{cell} and GAIR were independently calculated for each experiment using equation (2) (figure 3). The mean absolute value for rat liver GAIR *in vivo* of ~ 18.5 k Ω cm is almost half the value calculated in our *in vitro* study (~ 37.2 k Ω cm) (one tail $p \leq 0.042$) (Golberg *et al* 2009b).

3.2. Effect of NTIRE treatment on GAIR values

Both pulse delivery and GAIR measurements were performed with the same set of Zn/Cu electrodes (figure 1). At the end of each NTIRE treatment, the pulse generator was replaced by a simple resistance unit and a voltmeter. Figure 4 shows that immediately after the NTIRE procedure, GAIR value went down by 33% compared with measurements obtained immediately before the treatment (one tail $p \leq 0.0068$).

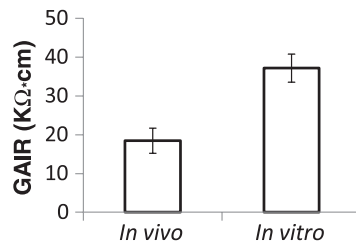


Figure 3. Rat liver GAIR. Mean absolute *in vivo* and *in vitro* GAIR values (Golberg *et al* 2009b). *In vitro* measurements were taken less than 1 h after the animal was sacrificed. The results are means of five replications. Error bar represents one standard deviation.

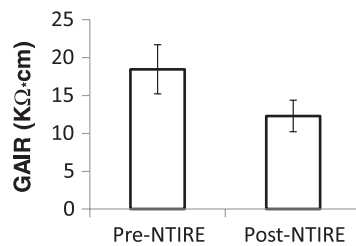


Figure 4. Effect of NTIRE on rat liver GAI. GAI measurement was performed immediately pre- and post-NTIRE *in vivo* treatment. The results are mean values of five replications. Error bar represents one standard deviation.

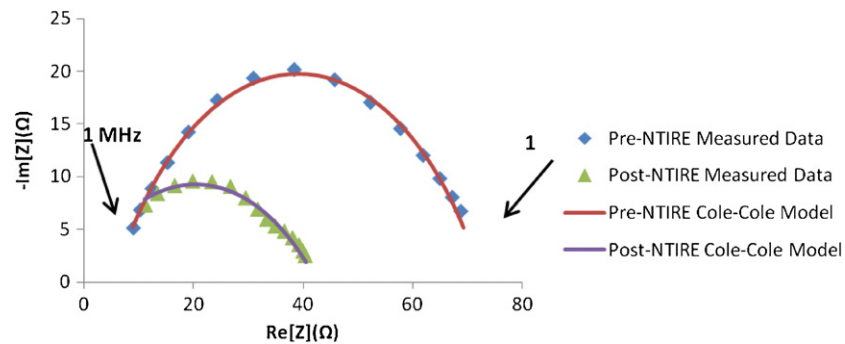


Figure 5. Wessel diagram of the impedance for the control and NTIRE treated rat liver. Measurements of ac impedance were performed before and after NTIRE *in vivo* treatment. The mean data of five measurements and the corresponding Cole–Cole models are presented.

3.3. Changes in ac bioimpedance in NTIRE treated liver

A Cole–Cole model was fitted for each measurement (figure 5). In a few cases, a partial secondary dispersion in the lower frequency range was evident. Therefore the analysis included 15 frequencies from 1 kHz to 1 MHz. The mean difference between the fitted model and the measured data before and after the NTIRE treatment was $0.4 \pm 0.2 \Omega$, i.e. $\sim 1.3\%$ (figure 5).

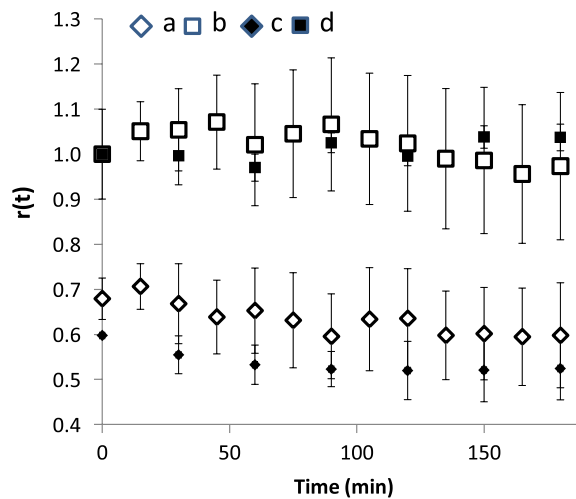


Figure 6. Time-dependent effect of a single NTIRE treatment on rat liver GAIR and R_0 . The plot represents the ratio $r(t)$ of: (a) NTIRE treated tissue GAIR at times t and t_0 ; (b) GAIR value of control tissue at times t and t_0 ; (c) R_0 value of NTIRE treated tissue at times t and t_0 ; (d) R_0 values of control tissue at times t and t_0 . Each point represents the mean of five replications. Error bar represents one standard deviation.

3.4. Long-term changes in GAIR and ac bioimpedance following NTIRE treatment of rat liver

GAIR and ac impedances of the treated and control livers were measured for 3 h after the single NTIRE treatment (figure 6). $R(t)$ represents the ratio between GAIR or R_0 values at time t to the respective values at $t_0 = 0$. The GAIR and R_0 values immediately post-NTIRE pulse sequence were 33% and 40% lower than the respective values measured just before the NTIRE treatment. In control animals, GAIR and R_0 of the liver remained unchanged. Three hours after the end of the NTIRE procedure, GAIR and R_0 were 40% and 47% lower than the pre-treated values, respectively, while GAIR and R_0 of the control animals' liver remained almost unchanged (figure 6).

Figure 7 shows the time-dependent changes in bioimpedance α and f_c parameters. On the initiation of the NTIRE treatment, an immediate 20% drop in α value was recorded ($p \leq 6.89 \times 10^{-5}$). With time, however, α value went up close to the original level. Following the initiation of the NTIRE treatment, f_c value increased by a factor of 6, and by a factor of 10, 30 min later.

3.5. Effect of NTIRE on tissue morphology

No visible injury or bleeding was observed in the control liver lobes sandwiched for 3 h between the Cu and Zn electrodes. In NTIRE treated livers, however, the contact surface between tissue and electrodes was dark red, due to RBC entrapping (figure 8 (Ivorra and Rubinsky 2007)). The latter tissues had also a marked increase in the inter-cell space, probably due to cell lysis (figure 8). Additionally, NTIRE treatment was followed by changes in cell structure. Hence, integrity loss of some hepatocytes was accompanied by certain changes in the cytoplasm. In contrast, eosinophilic color of control hepatocytes was similar to that of the cytoplasm due to the presence of numerous mitochondria, spots of free ribosomes and intact rough endoplasmic reticulum. Eosinophilia in NTIRE treated cells was lower than control, and hence the latter absorbed eosin dye more than treated cell cytoplasm, probably due to lysis of free ribosomes

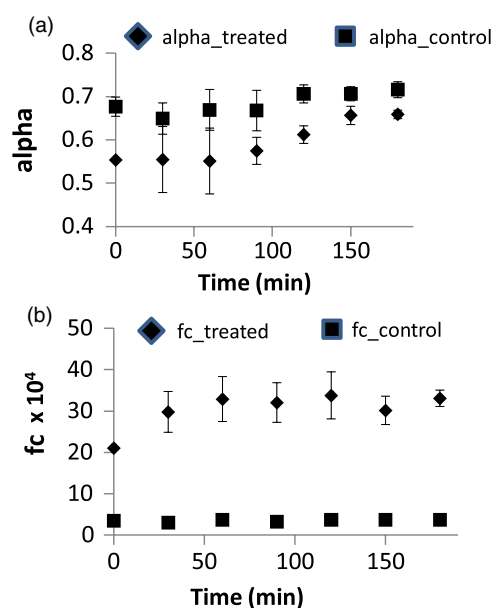


Figure 7. Long-term ac bioimpedance values. Measurements were taken by the four-electrode method. The following parameters derived from Cole–Cole fitted plot were recorded for 3 h following the single NTIRE treatment: (a) α parameter for NTIRE treated (α treated) and control (α control) tissues; (b) f_c parameter for NTIRE treated (f_c treated) and control (f_c control) tissues. Each point represents the mean of five replications. Error bar represents one standard deviation.

and/or damage caused by NTIRE to inner membranes including mitochondria and rough endoplasmic reticulum.

4. Discussion

The current study was undertaken to substantiate *in vivo* our previous findings that NTIRE treatment for cells' ablation is accompanied by typical changes in tissue GAIR values.

In control rats, a comparison between *in vitro* and *in vivo* GAIR properties shows that the values of the former for measurements taken less than 1 h after the animal was sacrificed (Golberg *et al* 2009b), are twice as high as those recorded *in vivo* (figure 3). The initial increase of GAIR may be due to cessation of blood flow with consequent cell swelling. Similar changes in ac bioimpedance in excised tissues were reported by others. For instance, Spottorno *et al* (2008) measured a twofold increase in electric resistivity in 50 Hz ac treated pigs' livers and kidneys, 2 h after the organ excision (Spottorno *et al* 2008). Haemmerich *et al* (2002) reported 62% and 24% increase in swine liver ac impedance at 1 and 500 kHz, respectively, after blood supply occlusion *in vivo* (Haemmerich *et al* 2002). Furthermore, during the first 2 h after excision, 53% and 32% increases in organ resistivity at 10 Hz and 1 MHz were recorded, respectively (Haemmerich *et al* 2002). Thereafter, decreases in the above two bioimpedance parameters were recorded, probably due to membrane disintegration.

Similarly, our *in vitro* studies showed a 25% decrease in GAIR within 2 h of the animals' death, from the initial *in vitro* value, from ~ 37.2 to ~ 28.9 k Ω cm (unpublished).

In control animals, the GAIR and ac resistivity differences between the *in vivo* and *in vitro* may result from the complete cessation of blood flow in the excised organ, with the consequent

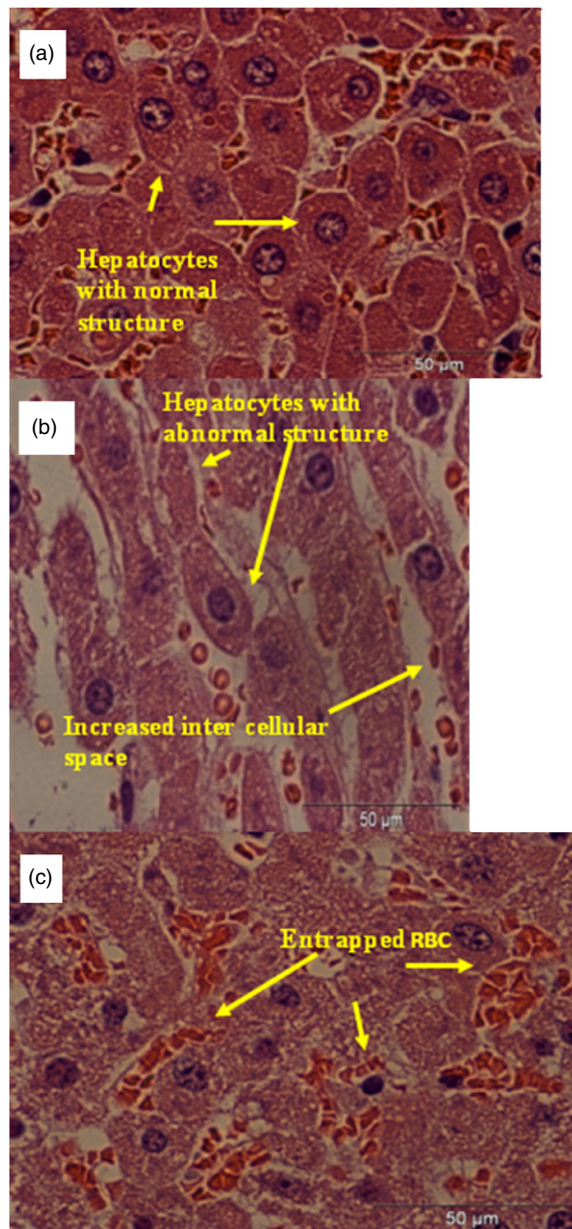


Figure 8. Histological images of rat livers (H&E X600): (a) control liver, removed after 3 h of continuous GAIR measurement; (b) and (c) NTIRE treated liver, removed 3 h after the treatment and continuous GAIR measurement. Treatment consisted of 90 unipolar, 70 μ s duration, 150 V mm^{-1} rectangular electrical pulses delivered at 4 Hz.

slow down in metabolism, as well as impairment and rupture of cells. Lysis processes in the excised tissue lead to increase in ion concentration (De Groot and Rauen 2007, Spottorno *et al* 2008), with the consequent decrease in GAIR as measured 2 h after excision.

Electroporation, a complex electrophysiological process, involves the interaction of external electric fields with biological cells. The success of NTIRE procedure depends on location and biological factors (Ivorra *et al* 2009, Ivorra and Rubinsky 2007, Rubinsky 2010). As direct observations of cell damage by NTIRE during the treatment are not possible, the impact of NTIRE on tissue can be measured only by tracking changes in physico-chemical tissue properties.

A number of ac impedance-based methodologies were developed for evaluation/measurement of electroporation effect(s) on tissues (Ivorra *et al* 2009, Ivorra and Rubinsky 2007). These, however, require additional sophisticated and costly device(s) whereas both the pulse delivery and GAIR measurements employ the same set of Cu/Zn electrodes (figures 1 and 2). The GAIR-based measuring system is independent of external power, and provides a low cost and reliable tool for assessing the NTIRE effect *in vivo*.

In intact (control) tissues, effective diffusivity and GAIR remained unchanged (figures 4 and 8), whereas exposure to NTIRE pulses (figure 4) resulted in a significant reduction in the tissue's GAIR and R_0 values by 33% and 40% respectively, most probably due to membrane rupture and consequent cell death (figures 4 and 8). The drop in these two parameters may result in an increase in diffusivity effectiveness. Our data show that membrane rupture resulted in leach of the cellular contents (figure 8) with the consequent increase in ion concentration in the inter-cellular space. Earlier we proposed that ionic diffusivity through the salt bridge between electrodes is affected by tissue tortuosity, the basis for GAIR measurement (Golberg *et al* 2009b). The current results support our previous suggestion that cell death and the consequent increase of inter-cellular space (figure 8) lead to decrease in tissue tortuosity.

In NTIRE treated livers, we tested the long-term effects in GAIR and ac impedance values, for 3 h after treatment (Al-Sakere *et al* 2007, Edd *et al* 2006; figure 6). In comparison to values obtained just prior to the NTIRE treatment, the GAIR and R_0 values dropped significantly immediately after the electric pulses treatment and 3 h later by 33% to 40% (GAIR) and by 40% and 47% (R_0), respectively (figures 6(a) and (c)). A delay in cell death, continued cell lysis, and the consequent increase in tissue tortuosity may explain the decrease in GAIR and R_0 values during the 3 h incubation and the consequent changes in the electric current flow in the treated tissues. In the control tissues, the values of GAIR and R_0 remained unchanged (figures 6(b) and (d)).

Changes were also recorded in the α and f_c parameters (figure 7). Generally α indicates tissue heterogeneity due to differences in cell size and shape in living tissues (Ackmann and Seitz 1984, Foster *et al* 1993) and the extra-cellular space morphology (Ivorra *et al* 2005). Figure 8 shows changes in cell size, shape and in the intra-cellular spaces, between control and NTIRE treated tissues. The differences observed in α (figure 7(a)) probably occur due to additional cumulative changes in treated tissue. f_c values provide numerical indications as to cell membrane quantity and viability (Halter *et al* 2009); thus, the tenfold increase in f_c values within 30 min of the NTIRE treatment (figure 7(b)) reflects the anticipated effect of NTIRE on the cell membrane. Hence, the calculated changes in the two parameters support our proposed post-NTIRE processes in treated tissues.

5. Conclusions

Our findings support the initial hypothesis that certain NTIRE tissue ablation protocols induce significant and measurable changes in GAIR value. The proposed measuring technique requires a single pair of electrodes with specific chemical potentials, resulting from combined effect of the electrode's material basic properties and those of the tissue of interest.

Moreover, the technique can be applied independently of external calibrated power source, and thus used *in vivo* anywhere inside the body.

In conclusion, the change in GAIR in NTIRE tissues may be used in molecular surgery for NTIRE real-time feedback.

References

- Ackmann J J and Seitz M A 1984 Methods of complex impedance measurements in biologic tissue *Crit. Rev. Biomed. Eng.* **11** 281–311
- Al-Sakere B, Andre F, Bernat C, Connault E, Opolon P, Davalos R V, Rubinsky B and Mir L M 2007 Tumor ablation with irreversible electroporation *PLoS ONE* **2** e1135
- Barbosa-Cánovas G V, Gongora-Nieto M M, Pothakamury U R and Swanson B G 1999 *Preservation of Foods with Pulsed Electric Fields* (London: Academic)
- Cukjati D, Batiuskaite D, Andre F, Miklavcic D and Mir L M 2007 Real time electroporation control for accurate and safe *in vivo* non-viral gene therapy *Bioelectrochemistry* **70** 501–7
- De Groot H and Rauen U 2007 Ischemia-reperfusion injury: processes in pathogenetic networks: a review *Transplant. Proc.* **39** 481–4
- Dev S B, Dhar D and Krassowska W 2003 Electric field of a six-needle array electrode used in drug and DNA delivery *in vivo*: analytical versus numerical solution *IEEE Trans. Bio-Med. Eng.* **50** 1296–300
- Edd J F and Davalos R V 2007 Mathematical modeling of irreversible electroporation for treatment planning *Technol. Cancer Res. Treat.* **6** 275–86
- Edd J F, Horowitz L, Davalos R, Mir L M and Rubinsky B 2006 *In vivo* results of a new focal tissue ablation technique: irreversible electroporation *IEEE Trans. Biomed. Eng.* **53** 1409–15
- FDA 2000 Kinetics of microbial inactivation for alternative food processing technologies IFT/FDA Contract No 223-98-2333, US Food and Drug Administration Center for Food Safety and Applied Nutrition <http://www.cfsan.fda.gov/~comm/ift-pef.html>
- Foster K R and Schwan H P 1989 Dielectric properties of tissues and biological materials: a critical review *Crit. Rev. Biomed. Eng.* **17** 25–104
- Foster R, Bihrl R, Sanghvi N, Fry F J and Donohue J P 1993 High-intensity focused ultrasound in the treatment of prostatic disease *Eur. Urol.* **23** (Suppl. 1) 29–33
- Gabriel C and Gabriel S 1996 Compilation of the dielectric properties of body tissues at RF and microwave frequencies http://niremf.ifac.cnr.it/docs/DIELECTRIC/Report.html#Rev_of_Dielec_Prop_of_Tissues
- Gabriel C, Gabriel S and Corthout E 1996 The dielectric properties of biological tissues: I. Literature survey *Phys. Med. Biol.* **41** 2231–49
- Glahder J, Norrild B, Persson M B and Persson B R 2005 Transfection of HeLa-cells with pEGFP plasmid by impedance power-assisted electroporation *Biotechnol. Bioeng.* **92** 267–76
- Golberg A, Belkin M and Rubinsky B 2009a Irreversible electroporation for microbial control of drugs in solution *AAPS Pharm. Sci. Tech.* **10** 881–6
- Golberg A, Fischer Y and Rubinsky B 2010a The use of irreversible electroporation in food preservation *Irreversible Electroporation* ed B Rubinsky (Berlin: Springer) pp 273–312
- Golberg A, Rabinowitch H and Rubinsky B 2010b Zn/Cu-vegetative batteries, bioelectrical characterizations and primary cost analyses *J. Renew. Sustainable Energy* **2** 033103, also highlighted in *Nature* **465** 848
- Golberg A, Rabinowitch H D and Rubinsky B 2009b Galvanic apparent internal impedance: an intrinsic tissue property *Biochem. Biophys. Res. Commun.* **389** 168–71
- Grimnes S and Martinsen O 2000 *Bioimpedance and Bioelectricity Basics* (San Diego, CA: Elsevier)
- Guimerà A, Gabriel G, Parramon D, Calderón E and Villa R 2009 Portable 4 Wire Bioimpedance Meter with Bluetooth Link *World Congress on Medical Physics and Biomedical Engineering (Munich, Germany, 7–12 September 2009)* pp 868–71
- Guo Y, Zhang Y, Klein R, Nijm G M, Sahakian A V, Omary R A, Yang G Y and Larson A C 2010 Irreversible electroporation therapy in the liver: longitudinal efficacy studies in a rat model of hepatocellular carcinoma *Cancer Res.* **70** 1555–63
- Haemmerich D, Ozkan O R, Tsai J Z, Staelin S T, Tungjitkusolmun S, Mahvi D M and Webster J G 2002 Changes in electrical resistivity of swine liver after occlusion and postmortem *Med. Biol. Eng. Comput.* **40** 29–33
- Halter R J, Hartov A, Paulsen K D, Schned A and Heaney J 2008 Genetic and least squares algorithms for estimating spectral EIS parameters of prostatic tissues *Physiol. Meas.* **29** S111–23
- Halter R J, Schned A, Heaney J, Hartov A and Paulsen K D 2009 Electrical properties of prostatic tissues: II. Spectral admittivity properties *J. Urol.* **182** 1608–13

- Ivorra A, Al-Sakere B, Rubinsky B and Mir L M 2009 *In vivo* electrical conductivity measurements during and after tumor electroporation: conductivity changes reflect the treatment outcome *Phys. Med. Biol.* **54** 5949–63
- Ivorra A, Genesca M, Sola A, Palacios L, Villa R, Hotter G and Aguilo J 2005 Bioimpedance dispersion width as a parameter to monitor living tissues *Physiol. Meas.* **26** S165–73
- Ivorra A and Rubinsky B 2007 *In vivo* electrical impedance measurements during and after electroporation of rat liver *Bioelectrochemistry* **70** 287–95
- Kenneth S C and Robert H C 1941 Dispersion and absorption in dielectrics: I. Alternating current characteristics *J. Chem. Phys.* **9** 341–51
- Kiehne H A 2003 *Battery Technology Hand Book* 2 edn (New York: Dekker)
- Lee E W, Chen C, Prieto V E, Dry S M, Loh C T and Kee S T 2010 Advanced hepatic ablation technique for creating complete cell death: irreversible electroporation *Radiology* **255** 426–33
- Lee E W, Loh C T and Kee S T 2007 Imaging guided percutaneous irreversible electroporation: ultrasound and immunohistological correlation *Technol. Cancer Res. Treat.* **6** 287–94
- Lelieveld H L M, Notermans S and de Haan S W H 2007 *Food Preservation by Pulsed Electric Fields. From Research to Application* (Cambridge: CRC Press)
- Marquardt D W 1963 An algorithm for least-squares estimation of nonlinear parameters *J. Soc. Ind. Appl. Math.* **11** 431–41
- Mir L M 2001 Therapeutic perspectives of *in vivo* cell electropermeabilization *Bioelectrochemistry* **53** 1–10
- Moré J 1978 The Levenberg–Marquardt algorithm: implementation and theory *Num. Anal.* **630** 105–16
- Neumann E, Schaefer-Ridder M, Wang Y and Hofschneider P H 1982 Gene transfer into mouse lymphoma cells by electroporation in high electric fields *EMBO J.* **1** 841–5
- Rubinsky B 2007 Irreversible electroporation in medicine *Technol. Cancer Res. Treat.* **6** 255–60
- Rubinsky B 2010 *Irreversible Electroporation* (Berlin: Springer)
- Spottorno J, Multigner M, Rivero G, Alvarez L, de la Venta J and Santos M 2008 Time dependence of electrical bioimpedance on porcine liver and kidney under a 50 Hz ac current *Phys. Med. Biol.* **53** 1701–13
- Thomson K 2010 Human experience with irreversible electroporation *Irreversible Electroporation* ed B Rubinsky (Berlin: Springer) pp 249–54
- Vanysek P 2007 Electrochemical series *Handbook of Chemistry and Physics* 89th edn ed D R Lide (London: Taylor & Francis)